STRUCTURAL WEIGHT MINIMIZATION UNDER STRESS CONSTRAINTS AND MULTIPLE LOADING

RENATHA B. SANTOS, CINTHIA G. LOPES AND ANTONIO A. NOVOTNY

Abstract. In this paper we present an approach for structural weight minimization under von Mises stress constraints and multiple load-cases. The minimization problem is solved by using the topological derivative concept, which allows the development of efficient and robust topology optimization algorithms. Since we are dealing with multiple loading, the resulting sensitivity is obtained as a sum of the topological derivatives associated with each load-case. The derived result is used together with a level-set domain representation method to devise a topology design algorithm. Several numerical examples are presented showing the effectiveness of the proposed approach.

1. Introduction

Structural topology optimization has been deeply researched over the last decades and several approaches for topology optimization have already been proposed [13, 10, 1, 20, 21]. In particular, in the design of mechanical components, one of the most important requirement is to find the optimal configuration which satisfies a material failure criterion [22, 14, 4, 17, 11, 12]. A more realistic situation arises by considering that the structure is subjected to multiple load-cases [2, 15, 18]. In this paper we present an approach for structural weight minimization under stress constraints and multiple loading. The minimization problem we are dealing with is solved by using the topological derivative concept.

The topological derivative is defined through a limit passage when the small parameter governing the size of the topological perturbation goes to zero, so that it can be used as a steepest-descent direction in an optimization process like in any method based on the gradient of the objective functional. This concept was introduced in 1999 through the fundamental paper [23] and since then the topological derivative has been successfully applied for solving many relevant engineering problems, such as: topology optimization, inverse problems, imaging processing, multi-scale material design and mechanical modeling including damage and fracture evolution phenomena. However, according to the literature, there are only few papers dealing with the topological derivative in the context of structural topology optimization under stress constraints [7, 8], which consider only the case of single loading.

The idea here is to extend the work [7] by considering multiple load-cases. In particular, we propose a multiple loading topology optimization problem which consists in minimizing the weight of the structure under von Mises stress constraints. Since the topological derivative obeys the basic rules of the Differential Calculus [21], the resulting sensitivity is obtained as a sum of the topological derivatives associated with each load-case. In addition, the complicated formulas derived in [7] are revisited and presented in a simplified manner by considering only the limit cases when the contrast parameter governing the material properties of the topological perturbations goes to zero or infinity. The interested reader may refer to [9], where such limit cases are discussed together with the concept of degenerated topological derivative. Following the original ideas presented in [6], the simplified results are then used together with a level-set domain representation method to devise a multiple loading topology optimization algorithm. Finally, numerical examples associated with single as well as multiple loading are presented, showing the effectiveness of the proposed approach.

This paper is organized as follows. In Section 2 the topology optimization problem we are dealing with is stated together with the associated topological derivative. In Section 3 a multiple loading topology optimization problem is formulated. The resulting topology optimization algorithm is roughly described in Section 4. In Section 5 some numerical results are presented. Finally, the paper ends with some concluding remarks in Section 6.

2. Problem statement

The idea of this paper is to minimize the weight of two-dimensional elastic structures under plane stress or plane strain assumptions, subject to von Mises stress constraints and multiple loading. In order to simplify the presentation, in this section we consider the topology optimization problem associated with a single loading. The obtained result is then extended to the case of multiple loading in Section 3.

2.1. **The constrained topology optimization problem.** Let us consider an open and bounded domain $\mathcal{D} \subset \mathbb{R}^2$ and a sub-domain $\Omega \subset \mathcal{D}$ with Lipschitz boundary Γ. See sketch in Fig. 1. The boundary Γ is the union of three given non-overlapping subsets, namely, Γ_D, Γ_N and Γ_0. On Γ_D the displacements are prescribed, while the non-zero and zero boundary tractions are prescribed on Γ_N and Γ_0, respectively. The idea is to minimize the weight of the structure under local stress constraints. Since this problem is ill-posed, a regularization term given by the strain energy stored in the structure is included [3]. However, it is not sufficient to control the complexity of the resulting topologies. For more sophisticated structural complexity control, the reader may refer to [19], for instance. The resulting constrained topology optimization problem is written as follows. Given a hold-all domain $\mathcal{D}$ and a stress constraints-enforcement subdomain $\Omega^\star \subset \mathcal{D}$, find $\Omega = (\Omega^\star \cup \omega) \subset \mathcal{D}$

Date: July 22, 2020.

Key words and phrases. Topology Optimization; Topological Derivative; Multiple Load-Cases; von Mises stress constraints.

that solves:

$$\left\{\begin{array}{l}\underset{\Omega\subset\mathcal{D}}{\text{Minimize}}\ \mathcal{J}_\Omega := |\Omega| + \kappa\mathcal{K}_\Omega,\\ \text{subject to}\quad \sigma_M \le \overline{\sigma}\quad \text{a.e. in}\quad \Omega^\star \subset \Omega,\end{array}\right. \tag{2.1}$$

where $\kappa > 0$, $\overline{\sigma}$ is the stress limit and ω is used to denote a part of Ω where the stress constrains are not enforced. The compliance $\mathcal{K}_\Omega$ is defined as

$$\mathcal{K}_\Omega := \mathcal{K}_\Omega(u) = \int_{\Gamma_N} q\cdot u, \tag{2.2}$$

where the vector function u is solution to the following boundary value problem:

$$\left\{\begin{array}{rcll}\text{div}\sigma(u) &=& 0 & \text{in } \mathcal{D},\\ u &=& 0 & \text{on } \Gamma_D,\\ \sigma(u)n &=& q & \text{on } \Gamma_N,\\ \sigma(u)n &=& 0 & \text{on } \Gamma_0.\end{array}\right. \tag{2.3}$$

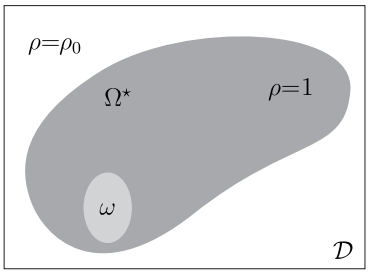

FIGURE 1. Hold-all domain.

Note that the stress constraint cannot usually be enforced, for example, in point loads. Then, we conveniently consider the sub-domain ω as a part of $\mathcal{D}$ that the stress constraints are not enforced. Some terms in the above equations still require explanations. In (2.1), $|\Omega|$ denotes the Lebesgue measure of Ω, i.e. the volume of the structure. The von Mises effective stress σ_M is written as:

$$\sigma_M := \sigma_M(u) = \sqrt{\frac{1}{2}\mathbb{B}\sigma(u)\cdot\sigma(u)}, \tag{2.4}$$

with

$$\mathbb{B} = 3\mathbb{I} - \mathrm{I}\otimes\mathrm{I}, \tag{2.5}$$

where $\mathbb{I}$ and I are the fourth and second order identity tensors, respectively. The linear constitutive equation is given by

$$\sigma(u) = \rho\mathbb{C}\varepsilon(u), \tag{2.6}$$

with the linearized Green tensor defined as follows

$$\varepsilon(u) = \frac{1}{2}(\nabla u + (\nabla u)^\top). \tag{2.7}$$

The elasticity tensor is written as

$$\mathbb{C} = 2\mu\mathbb{I} + \lambda(\mathrm{I}\otimes\mathrm{I}), \tag{2.8}$$

in which μ and λ are the Lamé's coefficients, both considered constants everywhere. In the plane stress assumption we have

$$\mu = \frac{E}{2(1+\nu)} \text{ and } \lambda = \frac{\nu E}{1-\nu^2}, \tag{2.9}$$

while in plane strain assumption they are

$$\mu = \frac{E}{2(1+\nu)} \text{ and } \lambda = \frac{\nu E}{(1+\nu)(1-2\nu)}, \tag{2.10}$$

where E is the Young's modulus and ν the Poisson's ratio. The statement of the minimization problem is completed with the definition of a piecewise constant function ρ, such that:

$$\rho(x) := \left\{\begin{array}{ll}1, & \text{if } x\in\Omega,\\ \rho_0, & \text{if } x\in\mathcal{D}\setminus\overline{\Omega},\end{array}\right. \tag{2.11}$$

with $\rho_0 \ll 1$ used to mimic voids. That is, the original structural problem, where the structure itself consists of the domain Ω of given elastic properties and the remaining part $\mathcal{D}\setminus\overline{\Omega}$ of the hold-all is empty (has no material), is approximated by means of the two-phase material distribution given by (2.11) over $\mathcal{D}$ where the empty region $\mathcal{D}\setminus\overline{\Omega}$ is occupied by a (very weak) material with Young's modulus, $\rho_0 E$, much lower than the given Young's modulus, E, of the elastic (strong) material.

2.2. **The penalized optimization problem.** Following the original ideas introduced in [7], the point-wise stress constraints from (2.1) are approximated by a class of von Mises stress penalty functional. Thus, let us define the nominal stress $S(u)$ as follows

$$S(u) := \frac{\sigma(u)}{\overline{\sigma}}. \tag{2.12}$$

Then, the von Mises stress constraints in terms of normalized stresses are stated as:

$$S_M^2(u) = \frac{1}{2}\mathbb{B}S(u)\cdot S(u) \le 1. \tag{2.13}$$

Now, let $\Phi : \mathbb{R}_+ \to \mathbb{R}_+$ be a nondecreasing function of class $\mathcal{C}^2$. We assume that the derivatives Φ' and Φ'' are bounded. Then, the penalty functional is defined as:

$$\mathcal{G}_\Omega := \mathcal{G}_\Omega(u) = \int_{\Omega^\star} \Phi(S_M^2(u)). \tag{2.14}$$

In particular, we shall adopt a function Φ of the following functional form:

$$\Phi(t) \equiv \Phi_p(t), \tag{2.15}$$

where $p \ge 1$ is a given real parameter and $\Phi_p : \mathbb{R}_+ \to \mathbb{R}_+$ is defined as [4]

$$\Phi_p(t) = [1 + t^p]^{1/p} - 1. \tag{2.16}$$

Therefore, the original constrained optimization problem (2.1) can be approximated by the following unconstrained penalized optimization problem:

$$\underset{\Omega\subset\mathcal{D}}{\text{Minimize}}\ \mathcal{J}_\Omega^\alpha := \mathcal{J}_\Omega + \alpha\mathcal{G}_\Omega, \tag{2.17}$$

with the scalar $\alpha > 0$ used to denote a given penalty coefficient and u solution to (2.3). In order to simplify further analysis, let us introduce an adjoint state v, which is solution to the following boundary value problem:

$$\left\{\begin{array}{rcll}-\text{div}(\sigma(v)) &=& \text{div}(\chi_{\Omega^\star}k_1(u)\widetilde{\mathbb{B}}S(u)) & \text{in } \mathcal{D},\\ \sigma(v) &=& \rho\mathbb{C}\varepsilon(v) & \\ v &=& 0 & \text{on } \Gamma_D,\\ \sigma(v)n &=& -\chi_{\Omega^\star}k_1(u)\widetilde{\mathbb{B}}S(u)n & \text{on } \Gamma_N\cup\Gamma_0,\end{array}\right. \tag{2.18}$$

where the tensor $\widetilde{\mathbb{B}}$ is given by

$$\widetilde{\mathbb{B}} = 6\mu\mathbb{I} + (\lambda - 2\mu)\mathrm{I}\otimes\mathrm{I}. \tag{2.19}$$

The characteristic function $\chi_{\Omega^\star}$ is written as

$$\chi_{\Omega^\star} = \left\{\begin{array}{ll}1, & \text{in } \Omega^\star,\\ 0, & \text{otherwise.}\end{array}\right. \tag{2.20}$$

Finally, the function $k_1(u)$ is defined as

$$k_1(u) = \Phi'(S_M^2(u)). \tag{2.21}$$

2.3. **Topological derivative.** For the sake of completeness, the topological derivative associated with the shape functional $\mathcal{J}^{\alpha}_{\Omega}(u)$, derived in [7], is stated here in its closed form. Since we are using a very complacent material to mimic voids, the topological derivatives are presented in their limit cases versions when the contrast parameter governing the material properties of the topological perturbations goes to zero or infinity. Finally, the results are written in terms of the Lamé's coefficients, so that they can be used either in plane stress or plane strain assumptions.

Theorem 1. *The topological derivative of the shape functional $\mathcal{J}^{\alpha}_{\Omega}(u)$, defined in* (2.17)*, with respect to the nucleation of a small circular inclusion with different material property from the background, is given by the sum*

$$D_T\mathcal{J}^{\alpha}_{\Omega}(x) = D_T|\Omega|(x) + \kappa D_T\mathcal{K}_{\Omega}(x) + \alpha D_T\mathcal{G}_{\Omega}(x), \quad \forall x \in \mathcal{D}. \quad (2.22)$$

We are interested into two particular cases, which are:

Case 1. *Let us consider $x \in \Omega$. In this case $\rho = 1$ and the contrast on the material property goes to zero since $\rho_0 \ll 1$. Then the topological derivative $D_T\mathcal{G}_{\Omega}$ of the von Mises penalty functional reads*

$$D_T\mathcal{G}_{\Omega} = -\mathbb{P}_0 S(u)\cdot\varepsilon(v) - \chi_{\Omega^\star}k_1(u)\mathbb{TB}S(u)\cdot S(u) + \frac{1}{4}\chi_{\Omega^\star}k_1(u)(10S(u)\cdot S(u) - 2\mathrm{tr}^2 S(u)) + \chi_{\Omega^\star}\Psi(S(u)) - \chi_{\Omega^\star}\Phi(S^2_M(u)), \quad (2.23)$$

where the displacement field u is solution to (2.3) *while v solves the adjoint problem* (2.18)*. The polarization tensor $\mathbb{P}_0$ is given by*

$$\mathbb{P}_0 = \frac{\lambda+2\mu}{\lambda+\mu}\left(2\mathbb{I} - \frac{\mu-\lambda}{2\mu}\mathrm{I}\otimes\mathrm{I}\right), \quad (2.24)$$

while the fourth order tensor $\mathbb{T}$ is written as

$$\mathbb{T} = a_2\mathbb{I} + \frac{a_1-a_2}{2}\mathrm{I}\otimes\mathrm{I}, \quad (2.25)$$

with

$$a_1 = \frac{\lambda+\mu}{\mu}; \quad a_2 = \frac{\lambda+3\mu}{\lambda+\mu}. \quad (2.26)$$

The function $\Psi(S(u))$ can be written as

$$\Psi(S(u)) = \frac{1}{\pi}\int_0^1\int_0^{\pi}\frac{1}{t^2}\left[\Phi(S^2_M(u)+\Lambda(t,\theta)) - \Phi(S^2_M(u)) - \Phi'(S^2_M(u))\Lambda(t,\theta)\right]d\theta dt, \quad (2.27)$$

where

$$\Lambda(t,\theta) = -\frac{t}{2}\left[5(S^2_I - S^2_{I\!I})\cos\theta + 3(S_I - S_{I\!I})^2(2-3t)\cos 2\theta\right] + \frac{t^2}{4}\left[3(S_I+S_{I\!I})^2 + (S_I-S_{I\!I})^2(3(2-3t)^2 + 4\cos^2\theta) + 6(S^2_I - S^2_{I\!I})(2-3t)\cos\theta\right], \quad (2.28)$$

with S_I and $S_{I\!I}$ used to denote the eigenvalues of $S(u)$. Finally, the topological derivative of $\mathcal{K}_{\Omega}(u)$ is given by

$$D_T\mathcal{K}_{\Omega} = -\mathbb{P}_0\sigma(u)\cdot\varepsilon(u), \quad (2.29)$$

and the topological derivative of the volume reads

$$D_T|\Omega| = -1. \quad (2.30)$$

Case 2. *Now, let us consider $x \in \mathcal{D}\backslash\overline{\Omega}$. In this case $x \notin \Omega^\star$ by definition and $\rho = \rho_0 \ll 1$. Therefore, the contrast on the material property goes to infinity. Then the last term in* (2.22)*, namely $D_T\mathcal{G}_{\Omega}$, is given by*

$$D_T\mathcal{G}_{\Omega} = -\mathbb{P}_{\infty}S(u)\cdot\varepsilon(v), \quad (2.31)$$

with u and v solutions to (2.3) *and* (2.18)*, respectively. The polarization tensor $\mathbb{P}_{\infty}$ is written as*

$$\mathbb{P}_{\infty} = -\frac{\lambda+2\mu}{\lambda+3\mu}\left(2\mathbb{I} + \frac{\mu-\lambda}{2(\lambda+\mu)}\mathrm{I}\otimes\mathrm{I}\right). \quad (2.32)$$

The topological derivative of $\mathcal{K}_{\Omega}(u)$ is given by

$$D_T\mathcal{K}_{\Omega} = -\mathbb{P}_{\infty}\sigma(u)\cdot\varepsilon(u), \quad (2.33)$$

and, finally, the topological derivative of the volume assumes

$$D_T|\Omega| = 1. \quad (2.34)$$

Remark 2. *The topological derivative with respect to the nucleation of a small circular inclusion with different material property from the background, governed by a general contrast, can be found in* [7]*. The intermediate case when the contrast on the material properties is close to one can be applied in the context of mixture between different materials of close Young modulus, for instance. These ideas have been used in* [16] *for the design of bi-metallic devices purpose. Of course, when the contrast is equal to one, there is no topological perturbation and hence the topological derivative vanishes.*

3. The multiple loading topology optimization problem

In order to deal with structural weight minimization under local stress constraints and subject to a number NLC of load-cases, let us introduce the following multiple loading topology optimization problem, which can be stated as:

$$\underset{\Omega\subset\mathcal{D}}{\text{Minimize}}\ \mathcal{F}^{\alpha}_{\Omega} := |\Omega| + \kappa\sum_{\ell=1}^{\text{NLC}}\mathcal{K}^{\ell}_{\Omega} + \alpha\sum_{\ell=1}^{\text{NLC}}\mathcal{G}^{\ell}_{\Omega}, \quad (3.1)$$

with $\mathcal{K}^{\ell}_{\Omega} = \mathcal{K}_{\Omega}(u_\ell)$ and $\mathcal{G}^{\ell}_{\Omega} = \mathcal{G}_{\Omega}(u_\ell)$, where u_ℓ is the solution associated with the ℓ-th loading q_ℓ, namely

$$\begin{cases} \mathrm{div}\sigma(u_\ell) = 0 & \text{in } \mathcal{D},\\ u_\ell = 0 & \text{on } \Gamma_D,\\ \sigma(u_\ell)n = q_\ell & \text{on } \Gamma_N,\\ \sigma(u_\ell)n = 0 & \text{on } \Gamma_0. \end{cases} \quad (3.2)$$

Since the topological derivative concept satisfies the basic rules of the Differential Calculus [21], we have

$$D_T\mathcal{F}^{\alpha}_{\Omega}(x) = D_T|\Omega|(x) + \kappa\sum_{\ell=1}^{\text{NLC}}D_T\mathcal{K}^{\ell}_{\Omega}(x) + \alpha\sum_{\ell=1}^{\text{NLC}}D_T\mathcal{G}^{\ell}_{\Omega}(x), \quad \forall x\in\mathcal{D}, \quad (3.3)$$

where $D_T|\Omega|$ is the topological derivative of the volume, while $D_T\mathcal{K}^{\ell}_{\Omega}$ and $D_T\mathcal{G}^{\ell}_{\Omega}$ are respectively the topological derivatives of the compliance and of the penalty functional, both associated with the ℓ-th loading. See Theorem 1 for details. Therefore, the topological derivative of problem (3.1) is obtained as a sum of the sensitivities associated with each load-case. The derived result (3.3) is used together with a level-set domain representation method for solving the penalized problem (3.1). The resulting topology optimization algorithm is roughly explained in Section 4 for the reader convenience. For more details we refer to the original paper by Amstutz & Andrä [6].

4. The topology optimization algorithm

In this section a topology optimization algorithm based on the topological derivative together with a level-set domain representation method is presented. It has been proposed in [6] and consists basically in looking for a local optimality condition for the minimization problem (3.1), written in terms of the topological derivative and a level-set function.

Let us characterize the elastic part Ω as well as the complacent material $\mathcal{D}\setminus\overline{\Omega}$ by a level-set function $\psi \in L^2(\mathcal{D})$ of the form:

$$\Omega = \{x \in \mathcal{D};\, \psi(x) < 0\},\ \mathcal{D}\setminus\overline{\Omega} = \{x \in \mathcal{D};\, \psi(x) > 0\}. \quad (4.1)$$

where ψ vanishes on the interface between the two phases material. Note that sign of the level-set function is not standard [6]. However, it is just a sign convection without any particular consequence.

A local optimality condition for the multiple loading optimization problem (3.1), under the considered class of domain perturbation given by circular inclusions, can be stated as:

$$D_T\mathcal{F}^{\alpha}_{\Omega}(x) > 0,\ \forall x \in \mathcal{D}. \quad (4.2)$$

Such a local optimality condition has been rigorously derived by Amstutz in [5]. Therefore, let us define the quantity

$$g(x) := \begin{cases} -D_T\mathcal{F}^{\alpha}_{\Omega}(x), & \text{if } \psi(x) < 0, \\ D_T\mathcal{F}^{\alpha}_{\Omega}(x), & \text{if } \psi(x) > 0. \end{cases} \quad (4.3)$$

From (4.3), one can rewrite the condition (4.2) in the following equivalent form

$$\begin{cases} g(x) < 0, & \text{if } \psi(x) < 0, \\ g(x) > 0, & \text{if } \psi(x) > 0. \end{cases} \quad (4.4)$$

We observe that the condition (4.4) is satisfied whether the quantity g coincides with the level-set function ψ up to a strictly positive number, namely

$$\exists\, \tau > 0 : g = \tau\psi. \quad (4.5)$$

Therefore,

$$\theta := \arccos\left[\frac{\langle g, \psi\rangle_{L^2(\mathcal{D})}}{\|g\|_{L^2(\mathcal{D})}\|\psi\|_{L^2(\mathcal{D})}}\right] = 0, \quad (4.6)$$

which shall be used as optimality condition in the topology design algorithm, where θ is the angle between the functions g and ψ in $L^2(\mathcal{D})$.

Let us now explain the algorithm. We first choose an initial level-set function $\psi_0 \in L^2(\mathcal{D})$. In particular, a detailed explanation on the numerical discretization of the level-set function can be found in the original paper [6]. In a generic iteration n, we compute function g_n associated with the level-set function $\psi_n \in L^2(\mathcal{D})$. Thus, the new level-set function ψ_{n+1} is updated according to the following linear combination between the functions g_n and ψ_n, explicitly given by

$$\psi_{n+1} = \frac{1}{\sin\theta_n}\left[\sin((1-w)\theta_n)\psi_n + \sin(w\theta_n)\frac{g_n}{\|g_n\|_{L^2(\mathcal{D})}}\right], \quad (4.7)$$

where θ_n is the angle between g_n and ψ_n according to (4.6), and w is a step size determined by a line-search performed in order to decrease the value of the objective function $\mathcal{F}^{\alpha}_{\Omega_n}$, with Ω_n used to denote the elastic part associated to ψ_n. The step size w is initialized as $w = 1$. While $\mathcal{F}^{\alpha}_{\Omega_{n+1}} \geq \mathcal{F}^{\alpha}_{\Omega_n}$, the step size is updated as follows $w \leftarrow w/2$. Otherwise, if $\mathcal{F}^{\alpha}_{\Omega_{n+1}} < \mathcal{F}^{\alpha}_{\Omega_n}$, the topology is updated according to the new level-set function ψ_{n+1}. The process ends when the condition $\theta_n \leq \epsilon_\theta$ is satisfied in some iteration, where ϵ_θ is a given small numerical tolerance. The function ψ_0 is chosen as an unit vector of $L^2(\mathcal{D})$ and by construction $\psi_{n+1} \in \mathcal{S},\ \forall n \in \mathbb{N}$, so that the algorithm becomes numerically well conditioned. If at some iteration n the line-search step size w is found to be smaller then a given numerical tolerance $\epsilon_w > 0$ and the optimality condition is not satisfied, namely $\theta_n > \epsilon_\theta$, then a mesh refinement of the hold-all domain $\mathcal{D}$ is carried out and the iterative process is continued. The above procedure written in the form of a pseudo-code format can be found in [18], for instance.

5. Numerical examples

Since we are dealing with multiple loading, two situations denoted by C1 and C2 are considered. In the first case (C1), the loads are applied simultaneously (single loading) and the associated topological derivative is evaluated. On the other hand, in the second case (C2), the loads are applied separately (multiple loading) and the resulting sensitivity is obtained as a sum of the topological derivatives associated with each load-case.

In the following numerical examples the stopping criterion and the optimality threshold are given respectively by $\epsilon_w = 10^{-2}$, $\epsilon_\theta = 1^\circ$. Furthermore, the mechanical problem is discretized into linear triangular finite elements and three steps of uniform mesh refinement were performed during the iterative process. In addition, we assume that the structures are under plane stress assumption. The material property threshold is set as $\rho_0 = 10^{-3}$. The Young's modulus is given by $E = 4 \times 10^4$ and the Poisson's ratio is set as $\nu = 0.3$, while $p = 32$ in (2.16). We set the hold-all domain as initial guess, namely $\Omega = \mathcal{D}$. The domains $\Omega^\star$ and ω are represented by medium and light grays, respectively. Finally, the thick lines represent clamped boundary conditions.

The numerical realizations are driven as follows. We start by setting the stress constraints penalty parameter $\alpha = 0$. In this case the optimization problem (3.1) degenerates itself to volume minimization under compliance constraint, where κ represents a penalty parameter associated with the compliance. Therefore, we set κ such that a given amount of strain energy is stored by the resulting structure. Then, the process is restarted with the same κ, while the parameter α is turn-on and chosen so that the stress constraints are satisfied.

5.1. **Example 1: Tower.** Let us consider the topology design of a tower [6]. The hold-all domain is given by a T-bracket structure clamped on the bottom, which is discretized into a mesh containing 20164 elements and 10243 nodes. The stress limit is set as $\overline{\sigma} = 30$ and the loading consists of two pairs of forces $q_{1,3} = (-\sqrt{2}/2, -\sqrt{2}/2)$ and $q_{2,4} = (\sqrt{2}/2, -\sqrt{2}/2)$ applied at the two opposites bottom corners of the horizontal branch, as shown in Fig. 2. Finally, we choose $\kappa = 400$.

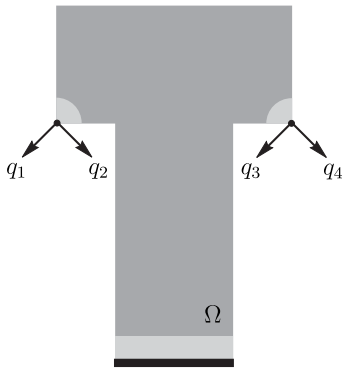

FIGURE 2. Tower. Initial guess and boundary conditions.

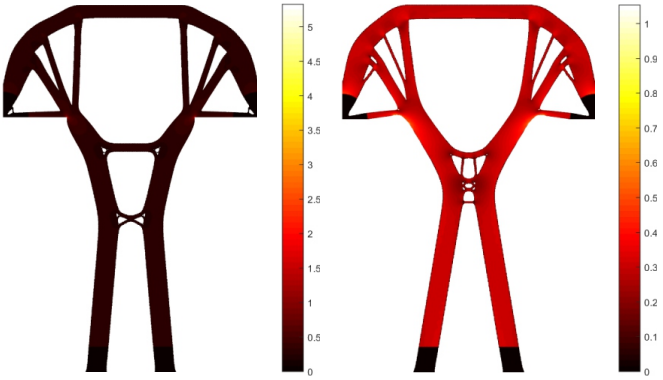

(a) (b)

FIGURE 4. Tower. Von Mises stress distribution for C1: (a) unconstrained case and (b) constrained case.

We first present the results for single loading, C1. The optimal topology in the unconstrained case ($\alpha = 0$) has been obtained after 65 iterations and it is present in Fig. 3(a). The resulting topology has approximately 33% of volume fraction. In the constrained case ($\alpha = 4 \times 10^4$) the final topology is presented in Fig. 3(b). This result has been obtained after 66 iterations with approximately 35% of volume fraction.

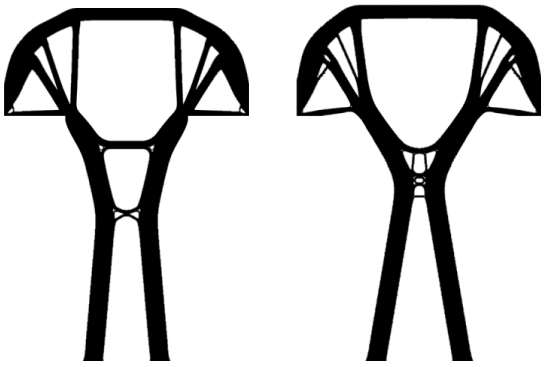

(a) (b)

FIGURE 3. Tower. Obtained results for C1: (a) unconstrained case and (b) constrained case.

Now, in Fig. 4 the stress distribution obtained at the end of the optimization process are presented. Note that in the unconstrained case, Fig. 4(a), the maximum stress clearly exceeds the threshold due to the domain singularity. On the other hand, in the constrained case, Fig. 4(b), the stress is under control and the reentrant corner is rounded unlike what occurs in the first case, Fig. 4(a). Besides, in this case, the maximum normalized stress is given by 1.05.

Now, we consider the multiple load-cases, C2. The optimal topologies obtained are those presented in Figs. 5(a) and 5(b). The final topology in the unconstrained case ($\alpha = 0$) has been obtained after 43 iterations and has approximately 54% of volume fraction. In the constrained case ($\alpha = 1 \times 10^4$) the optimal topology has been obtained after 29 iterations with approximately 57% of volume fraction.

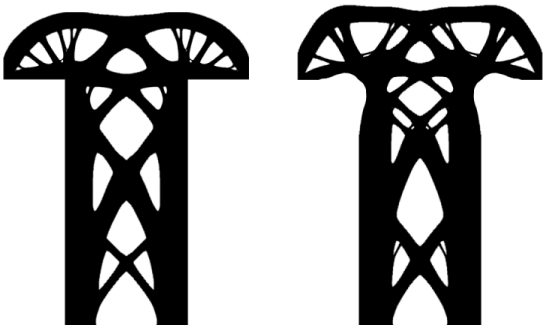

(a) (b)

FIGURE 5. Tower. Obtained results for C2: (a) unconstrained case and (b) constrained case.

The von Mises stress distribution corresponding to the loads $\ell = 1, 2$ obtained at the end of the optimization process are shown in Figs. 6 and 7. By symmetry of the load-cases, the solutions associated with $\ell = 3, 4$ are not presented. Once again, in the unconstrained case the maximum stress for each load exceeds the threshold. On the order hand, in the constrained case the stress remains under control for each load, see Table 1. In this case the reentrant corner is also rounded. Although the stress constraints are satisfied for each load we observe that the result is too conservative, that is, the optimal design is far to be fully stressed. Finally, the graphic in Fig. 8 shows the convergence curves of the shape functional (3.1) and the volume fraction.

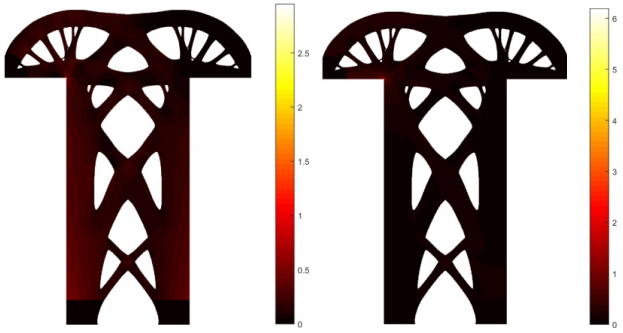

(a) $\ell = 1$ (b) $\ell = 2$

FIGURE 6. Tower. Von Mises stress distribution for C2: unconstrained case.

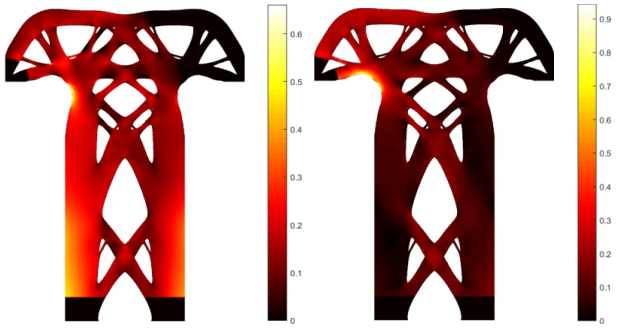

(a) $\ell = 1$ (b) $\ell = 2$

FIGURE 7. Tower. Von Mises stress distribution for C2: constrained case.

TABLE 1. Tower. Maximal normalized stress for C2 obtained at the end of the iterative process.

	Constrained Case
$\ell = 1, 4$	0.66
$\ell = 2, 3$	0.94

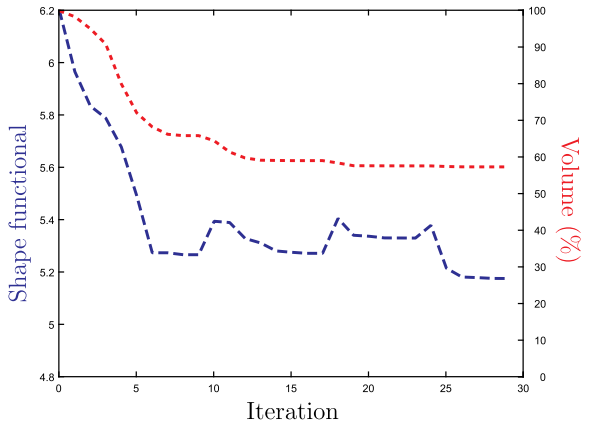

FIGURE 8. Tower. Shape functional and volume fraction for C2 during the iterative process: constrained case.

5.2. **Example 2: Wheel.** This example considers the design of an alloy wheel [18]. The hold-all domain is given by a ring of radii 0.2 and 1.0. The dark gray strip remains unchanged during the optimization process. The wheel is clamped on the smaller holes (little circles of radius 0.04). A uniformly distributed shear load q_9 of intensity 3.0 and eight normal loads q_i, $i = 1, ..., 8$, of intensity 7.0 are applied on the external boundary of the wheel. All the details are presented in Fig. 9. The multiple load-cases, C2, allow for a more realistic combination of the applied forces [15, 18]. Thus, in this example, only results for multiple loading are presented. The wheel is modeled using an initial mesh with 2048 elements and 1089 nodes. Finally, we set the stress limit as $\overline{\sigma} = 40$ and we chose $\kappa = 20$.

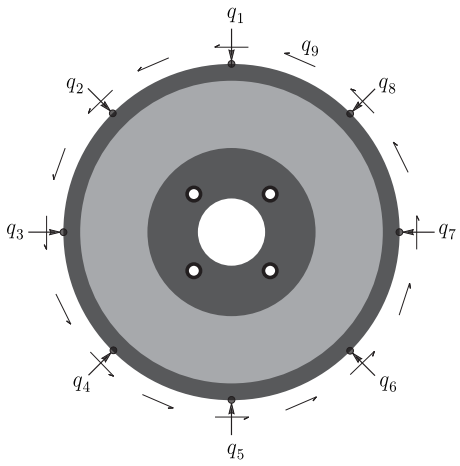

FIGURE 9. Wheel. Initial guess and boundary conditions.

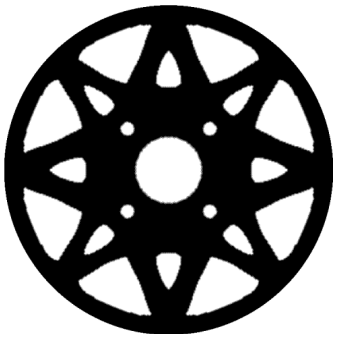

(a)

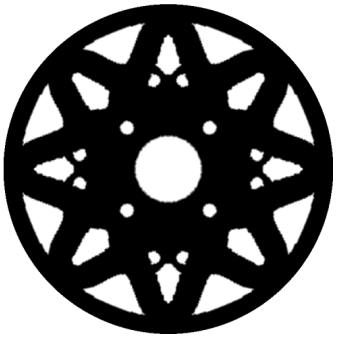

(b)

FIGURE 10. Wheel. Obtained results: (a) unconstrained case and (b) constrained case.

Fig. 10 presents the optimal topologies considering multiple loading for the unconstrained and constrained cases. The result for unconstrained case ($\alpha = 0$) has been obtained after 7 iterations, see Fig. 10(a). The maximum stress exceeds the admissible threshold for each load, as can be seen in Table 2. On the other hand, in the constrained case ($\alpha = 100$) the stress remains under control, as shown in Table 2. In this case, the result has also been obtained after 7 iterations, see Fig. 10(b). Finally, the volume fraction of the structures are approximately 71% and 80% respectively.

TABLE 2. Wheel. Maximal normalized stress obtained at the end of the iterative process.

	Unconstrained Case	Constrained Case
$\ell = 1, 3, 5, 7$	1.24	1.04
$\ell = 2, 4, 6, 8$	1.38	1.02
$\ell = 9$	1.08	0.87

6. Conclusion

In this paper the topological derivative concept has been applied in the context of structural weight minimization under von Mises stress constraints and multiple load-cases. Since the topological derivative obeys the basic rules of the Differential Calculus, the resulting sensitivity was obtained as a sum of the topological derivatives associated with each load-case. In addition, the topological derivative is defined through a limit passage when the small parameter governing the size of the topological perturbation goes to zero. Then, it can be used as a steepest-descent direction in an optimization process like in any method based on the gradient of the cost functional. In fact, the *exact* analytical formula for the topological sensitivity allows us to obtain the optimal designs in few iterations by using a minimal number of user defined algorithmic parameters, as shown in the numerical section. Finally, in contrast to traditional topology optimization methods, the topological derivative formulation does not require a material model concept based on intermediary densities, so that interpolation schemes are unnecessary. This feature is crucial in stress constrained problems, since the difficulties arising from material model procedures are here naturally avoided. Therefore, our approach can be seen as a simple alternative method for optimum design of structures under stress constraints and multiple loading.

Acknowledgements

This research was partly supported by CNPq (Brazilian Research Council), CAPES (Brazilian Higher Education Staff Training Agency) and FAPERJ (Research Foundation of the State of Rio de Janeiro). These supports are gratefully acknowledged.

References

[1] G. Allaire. *Conception optimale de structures*, volume 58 of *Mathématiques et applications*. Springer-Verlag, Berlin, 2007.

[2] G. Allaire and F. Jouve. A level-set method for vibration and multiple loads structural optimization. *Computer Methods in Applied Mechanics and Engineering*, 194(30-33):3269 – 3290, 2005.

[3] G. Allaire, F. Jouve, and H. Maillot. Topology optimization for minimum stress design with the homogenization method. *Structural and Multidisciplinary Optimization*, 28(2-3):87–98, 2004.

[4] S. Amstutz. A penalty method for topology optimization subject to a pointwise state constraint. *ESAIM: Control, Optimisation and Calculus of Variations*, 16(3):523–544, 2010.

[5] S. Amstutz. Analysis of a level set method for topology optimization. *Optimization Methods and Software*, 26(4-5):555–573, 2011.

[6] S. Amstutz and H. Andrä. A new algorithm for topology optimization using a level-set method. *Journal of Computational Physics*, 216(2):573–588, 2006.

[7] S. Amstutz and A. A. Novotny. Topological optimization of structures subject to von Mises stress constraints. *Structural and Multidisciplinary Optimization*, 41(3):407–420, 2010.

[8] S. Amstutz, A. A. Novotny, and E. A. de Souza Neto. Topological derivative-based topology optimization of structures subject to Drucker-Prager stress constraints. *Computer Methods in Applied Mechanics and Engineering*, 233–236:123–136, 2012.

[9] S. Amstutz, A. A. Novotny, and N. Van Goethem. Topological sensitivity analysis for elliptic differential operators of order $2m$. *Journal of Differential Equations*, 256:1735–1770, 2014.

[10] M. P. Bendsøe and O. Sigmund. *Topology optimization. Theory, methods and applications*. Springer-Verlag, Berlin, 2003.

[11] M. Bruggi and P. Duysinx. Topology optimization for minimum weight with compliance and stress constraints. *Structural and Multidisciplinary Optimization*, 46(3):369–384, 2012.

[12] H. Emmendoerfer Jr. and E. A. Fancello. A level set approach for topology optimization with local stress constraints. *International Journal for Numerical Methods in Engineering*, 99:129–156, 2014.

[13] H. A. Eschenauer and N. Olhoff. Topology optimization of continuum structures: a review. *Applied Mechanics Reviews*, 54(4):331–390, 2001.

[14] E. A. Fancello. Topology optimization of minimum mass design considering local failure constraints and contact boundary conditions. *Structural and Multidisciplinary Optimization*, 32:229–240, 2006.

[15] E. A. Fancello and J. T. Pereira. Structural topology optimization considering material failure constraints and multiple load conditions. *Latin American Journal of Solids and Strucutures*, 1:3–24, 2003.

[16] S. M. Giusti and A. A. Novotny. Design of bi-metallic devices based on the topological derivative concept. *Mechanical Research Communication*, 65:1–8, 2015.

[17] C. Le, J. Norato, and T. Bruns. Stress-based topology optimization for continua. *Structural Multidisciplinary Optimization*, 41:605–620, 2010.

[18] C. G. Lopes, R. B. dos Santos, and A. A. Novotny. Topological derivative-based topology optimization of structures subject to multiple load-cases. *Latin American Journal of Solids and Structures*, 12:834–860, 2015.

[19] J. A. Norato, B. K. Bell, and D. Tortorelli. A geometry projection method for continuum-based topology optimization with discrete elements. *Computer Methods in Applied Mechanics and Engineering*, 293:306–327, 2015.

[20] J. A. Norato, M. P. Bendsøe, R. B. Haber, and D. Tortorelli. A topological derivative method for topology optimization. *Structural and Multidisciplinary Optimization*, 33(4–5):375–386, 2007.

[21] A. A. Novotny and J. Sokołowski. *Topological derivatives in shape optimization*. Interaction of Mechanics and Mathematics. Springer-Verlag, Berlin, Heidelberg, 2013.

[22] J. T. Pereira, E. A. Fancello, and C. S. Barcellos. Topology optimization of continuum structures with material failure constraints. *Structural and Multidisciplinary Optimization*, 26(1–2):50–66, 2004.

[23] J. Sokołowski and A. Żochowski. On the topological derivative in shape optimization. *SIAM Journal on Control and Optimization*, 37(4):1251–1272, 1999.

Laboratório Nacional de Computação Científica LNCC/MCT, Av. Getúlio Vargas 333, 25651-075 Petrópolis - RJ, Brasil.
Email address: {renatha,cinthia,novotny}@lncc.br